Pion-deuteron breakup reaction at 228 MeV

E. L. Mathie, V. Pafilis, G. M. Huber,* G. J. Lolos, S. I. H. Naqvi,
Z. Papandreou, and D. M. Yeomans
University of Regina, Regina, Saskatchewan, Canada S4S 0A2

M. Sevior, R. P. Trelle,† D. Ottewell, G. R. Smith, and D. Healey
TRIUMF, Vancouver, British Columbia, Canada V6T 2A3

H. Garcilazo‡
Institute für Theoretische Physik, Universität Hannover, D-3000 Hannover, Federal Republic of Germany
(Received 29 June 1989)

Momentum distributions of triple differential cross sections for the reaction $\pi d \rightarrow \pi pn$ have been measured for 36 final-state pion-proton angle pairs at 228 MeV incident pion energy. The data are compared with earlier experimental results and with recent few-body calculations. In the region of quasifree elastic scattering the cross sections are typically lower than theoretical values by up to 30%. In regions away from quasifree scattering the general trends of the data are generally described, with best agreement on the low-momentum side of the distributions and with differences between theory and experiment as large as a factor of 10 in the worst cases. Together with the corresponding comparisons for the pion-deuteron elastic scattering and absorption channels, this failing might be an indication of the need to broaden the conventional calculations, or of the need to recognize an explicit quark contribution.

I. INTRODUCTION

The set of reactions that collectively form the πNN system may be used to gauge the extent of our understanding of several important, fundamental processes of intermediate energy nuclear physics. These reactions include the simplest nuclear pion production and absorption reactions ($\pi d \leftrightarrow pp$), as well as the pion deuteron and NN elastic scattering processes. The strong coupling between channels of the πNN system, which is reflected in modern theoretical efforts,[1-5] ensures that a good theoretical description in any one of the channels is not simply fortuitous. Relatively minor failings in the general description might come to light in only one of the channels, and perhaps only in certain kinematical extremes. Typical theoretical descriptions of the pion-deuteron elastic scattering cross section, for example, are satisfactory at small angles but often fail in the large-angle region.[6,7] In addition comparisons between experiment and theory for pion-deuteron elastic scattering are less than satisfactory for some of the measured polarization observables in different kinematical regions.[8] Similarly typical descriptions of the analyzing power for the pion deuteron absorption reaction[9] are not satisfactory even though the cross sections for that channel are well described.[10] Another member of this interesting set of reactions that may be studied with incident pions is the pion-deuteron breakup reaction, $\pi d \rightarrow \pi pn$. In providing us with a three-body final state, nature enables systematic studies within one channel across a tremendous kinematical spread, which should be considered together with results from the two-body reaction channels.

The few-body framework for this set of reactions ensures that a good calculation may be performed, and that failings must be interpreted as shortcomings in the completeness of the conventional physics approach, or perhaps in some way as a reflection of quark degrees of freedom at intermediate energies. The later situation is desirable from the point of view of smoothing the transition from a conventional nuclear physics description at very low energies to a quark description appropriate at very high energies but difficult to realize because of the potentially awkward many-body problem and because of prejudices to retain a conventional description.

Recently a variety of experiments has dramatically improved our knowledge on the pion-deuteron breakup reaction. This generation of kinematically complete experiments (typically the final-state pion and proton were detected in coincidence and the proton momentum measured) was lead by a group from Rice university[11,12] who determined cross sections for 11 pion-proton angle pairs. Comparisons with a distorted wave impulse approximation (DWIA) calculation including corrections for the NN and πN final-state interactions become very unfavorable for cases with a neutron momentum greater than 40 MeV/c. This experimental work stimulated few-body calculations by Matsuyama[13] and by Garcilazo[14] that were closer to the data than the DWIA calculation, particularly in the region where the pion-proton subsystem invariant mass is in the mass region of the Δ^{++}.

The next major experimental effort, in which a great deal of data for this three-body channel were obtained, was performed at Schweizerisches Institut für Nuklearforschung (SIN). These measurements included vector analyzing powers and cross sections at 228 MeV.[15] In this first breakup experiment by the Karlsruhe group at

SIN, both observables were measured simultaneously using a specially constructed polarized target cell, with an attached background target, and an array of time-of-flight counters positioned to simultaneously measure 36 pion-proton angle pairs. Matsuyama subsequently performed new calculations to include the specific angles where data was taken and found[15] values of cross section in agreement with those of the experiment only in kinematical regions where the impulse process dominates. In a subsequent publication, measurements of the vector analyzing powers at 134, 180, and 228 MeV measured by the Karlsruhe group were compared with a relativistic Faddeev calculation by Garcilazo,[16] finding that the vector analyzing power, $iT11$ data often fall as much as two standard deviations below the calculation, particularly for low-proton momenta and large pion angles. After this initial experiment the Karlsruhe group measured additional cross sections with 228 and 294 MeV pions interacting in a solid deuterated polythene target.[17] The target thickness and background subtraction were more precise than in the first Karlsruhe experiment. These data in general compared favorably with the Garcilazo calculation at the time, however an error was subsequently discovered in the calculations such that the predictions plotted in that work needed to be multiplied by a factor of 2, turning a favorable comparison into an unfavorable one. In addition a correction, discussed in detail following, for the out-of-plane detector acceptance, must be applied to those experimental results, partially compensating for the effect of the error just noted. More recently the Karlsruhe group have extended their breakup reaction studies with additional measurements of the triple differential cross sections at 294 MeV (Ref. 18) and the vector analyzing powers at 134 and 228 MeV (Ref. 19) with particular attention to kinematical regions where the final-state interaction between the proton and neutron are critical. This new work used a cryogenic deuterium target for the cross-section part of the experiment.

The Rice University group have also extended their original work, with measurements chosen to focus on the reaction as the final state of an intermediate, two-body delta production reaction.[20] Their philosophy in this effort was to measure a limited number of angle pairs with good energy resolution to enable determination of the delta production two-body reaction at two center-of-mass angles. These data have been compared with multiple scattering calculations by Laget and Faddeev calculations by Garcilazo. The Faddeev calculations by Garcilazo typically overestimate the peak by 43%, even in the region of quasifree scattering.

The experiment discussed in this work was performed at TRIUMF in parallel with the most recent Karlsruhe and Rice experiments. The phase-space coverage of this new experiment complements the other experiments. In order to minimize the background, a cryogenic deuterium target was used. For all cases a large amount of data were collected, so that even in regions of phase space well away from the quasifree kinematics (either in angle or in proton momentum) adequate statistical precision could be achieved for a meaningful comparison with theory. The time-of-flight spectrometer array of counters, which was previously used in the tensor pion-deuteron scattering experiments[8] and which is very similar to the Karlsruhe detector array, was used in a mode allowing the simultaneous collection of data for 36 angle pairs. Somewhat more information per event was recorded on magnetic tape than the earlier Karlsruhe experiments, enabling extraction of an experimentally determined out-of-plane acceptance correction.

II. THEORY

The theoretical results, compared with the TRIUMF experimental results in the following were obtained using the relativistic Faddeev equations within the three-body helicity formalism.[21] In this formalism one constructs a linear combination of the three-body helicity states proposed originally by Wick,[22] such that the new basis states contain the familiar quantum numbers of a pair, l_i, s_i, j_i, where l_i is the orbital angular momentum, s_i is the spin, and j_i is the total angular momentum. In this convention a subscript i always refers to the pair of particles jk formed without particles i; except for the quantities k_i, τ_i, σ_i, and ν_i that represent the single-particle i momentum, isospin, spin, and helicity. An index of 1 refers to the pion and 2 and 3 refer to the two nucleons.

Thus, the resulting integral equations are similar in form to the nonrelativistic Faddeev equations, except that here both the space and the spin variables are treated in a fully relativistic way at every stage. A complete description of the three-body helicity formalism has been previously reported,[21] while the particular form of this formalism in the case of separable two-body amplitudes for the application to the kaon deuteron and pion-deuteron elastic and breakup reactions has been previously presented.[23,16] The basic features of these equations are described next.

The relativistic Faddeev equations for the pion-deuteron elastic scattering and breakup T matrices are written in terms of the momenta k_i of the three particles in the three-body center-of-mass frame, as

$$T_{i1}^{\alpha_i,\alpha_{10}}(k_i k_{10})=(1-\delta_{i1})B_{i1}^{\alpha_i,\alpha_{10}}(k_i,k_{10})+\sum_{j\neq i}\sum_{\alpha_j}\int_0^\infty \frac{k_j^2 dk_j}{2\omega_j(k_j)} B_{ij}^{\alpha_i,\alpha_j}(k_i,k_j)G_j^{\alpha_j}(s_j)T_{j1}^{\alpha_j,\alpha_{10}}(k_j,k_{10}) , \quad (1)$$

where a subscript 0 indicates an initial value of the quantity, and

$$s_j=[\sqrt{S}-\omega_j(k_j)]^2-k_j^2 \quad (2)$$

is the invariant mass squared of the pair that excludes particle j, since $\sqrt{S}$ is the total invariant mass of the system. $G_j^{\alpha_j}(s_j)$ is the propagator of the interacting pair that excludes particle j, while the driving terms B_{ij} are given by

$$B_{ij}^{\alpha_i,\alpha_j}(k_i,k_j)=\int_{-1}^{1} d\cos\chi\, A_{ij}^{\alpha_i,\alpha_j}(k_i,k_j,\cos\chi)\frac{g_i^{\alpha_i}(p_i)g_j^{\alpha_j}(p_j)}{2\omega_k(|\mathbf{k}_i+\mathbf{k}_j|)}\frac{\omega_i(k_i)+\omega_j(k_j)+\omega_k(|\mathbf{k}_i+\mathbf{k}_j|)}{S-[\omega_i(k_i)+\omega_j(k_j)+\omega_k(|\mathbf{k}_i+\mathbf{k}_j|)]^2+i\epsilon}\ , \tag{3}$$

where $\cos\chi=(\mathbf{k}_i\cdot\mathbf{k}_j)/(k_ik_j)$, $g_j^{\alpha_j}(p_i)$ and $g_i^{\alpha_i}(p_i)$ and $g_j^{\alpha_j}(p_j)$ are the form factors of the separable two-body amplitudes with p_i and p_j the magnitudes of the relative momenta of the pairs excluding single particles i and j, respectively, and

$$\begin{aligned}A_{ij}^{\alpha_i,\alpha_j}(k_i,k_j,\cos\chi)=&(-1)^{t_j+\tau_j-T}[(2t_i+1)(2t_j+1)(2j_i+1)(2j_j+1)]^{1/2}\\&\times W(\tau_j\tau_kT\tau_i;t_it_j)\sum_{\lambda_j\lambda_k}\sum_{\mu_k\mu_i}b_{\lambda_j\lambda_k}^{l_i,s_i,j_i}b_{\mu_k\mu_i}^{l_js_jj_j}(-1)^{\sigma_j-\nu_j+\sigma_k+\mu_k}d^J_{m_j-\nu_j,m_i-\nu_i}(\chi)d^{j_i}_{m_i,\lambda_j-\lambda_k}(\theta_i)\\&\times d^{j_j}_{m_j,\mu_k-\mu_i}(\theta_j)d^{\sigma_i}_{\nu_i,\mu_i}(\beta_i)d^{\sigma_j}_{\nu_j,\lambda_j}(\beta_j)d^{\sigma_k}_{\mu_k,\lambda_k}(\rho_k)\end{aligned} \tag{4}$$

with

$$b_{\lambda_j\lambda_k}^{l_is_ij_i}=[(2l_i+1)/(2j_i+1)]^{1/2}C_{0,\lambda_j-\lambda_k}^{l_is_ij_i}b_{\lambda_j,-\lambda_k}^{\sigma_j\sigma_ks_i}\ , \tag{5}$$

where J and T are the total angular momentum and total isospin of the three-body channel, and as just discussed, τ_i, σ_i, and ν_i are the isospin, spin, and helicity of particle i while l_i, s_i, j_i, t_i, and m_i are the orbital angular momentum, spin, total angular momentum, isospin, and helicity of the pair i (composed of particles j and k). The arguments of the rotation matrices χ, θ_i, θ_j, β_i, β_j, and ρ_k in Eq. (4), are the angles of the Wick triangle.[21,22]

The two-body input of the integral Eqs. (1)–(5) are the pion nucleon S_{11}, S_{13}, P_{11}, P_{31}, P_{13}, and P_{33} channels and the nucleon-nucleon $^3S_1$, $^3D_1$, and $^1S_0$ channels, which are represented by separable T matrices. In the case of the pion-nucleon channels, the on-shell experimental data is used directly to parametrize the two-body T matrices, so that the propagator of the interacting pair $G_j^{\alpha_j}(s_j)$ is given by

$$G_j^{\alpha_j}(s_j)=-\frac{4\sqrt{s_j}}{\pi p_{j0}[g_j^{\alpha_j}(p_{j0})]^2}\sin\delta(s_j)\exp i\delta(s_j)\ , \tag{6}$$

where δ as usual denotes a pion-nucleon phase shift, and p_{j0} is the on-shell momentum of the pion-nucleon pair:

$$p_{j0}^2=[s_j-(M+\mu)^2][s_j-(M-\mu)^2]/4s_j \tag{7}$$

and the form factors $g_j^{\alpha_j}(p_j)$ are taken to be

$$g_j^{\alpha_j}(p_j)=p_j^{l_j}/(\Lambda^2+p_j^2) \tag{8}$$

with $\Lambda=1$ GeV/c. The pion-nucleon on-shell amplitudes corresponding to the propagators[6] are known not only in the physical region $s_j>(M+\mu)^2$, but also in the unphysical region $0<s_j<(M+\mu)^2$, as a result of the application of crossing symmetry and fixed-t dispersion relations.[24–26] In the case of the nucleon nucleon $^3S_1-{}^3D_1$ channel, the unitary pole approximation[27] was applied to the deuteron wave function of the Paris potential.[28] Since the corresponding T matrix would be a solution of the nonrelativistic Lippmann-Schwinger equation, the minimal relativity transformation[29] was applied in order to make it a solution of the Blankenbecler-Sugar equation. Thus, the propagator $G_j^{\alpha_j}(s_j)$ is in this case

$$\frac{1}{G_j^{\alpha_j}(s_j)}=(E-E_d)\times\int_0^\infty p^2dp\frac{h_0^2(p)+h_2^2(p)}{(E_d-p^2/M)(E-p^2/M+i\epsilon)}\ , \tag{9}$$

where $E_d=-2.225$ MeV is the energy of the deuteron. The energy, E is related to the invariant mass squared s_j as

$$E=s_j/4M-M\ , \tag{10}$$

where M is the nucleon mass and the nonrelativistic form factors $h_l(p)$ are

$$h_l(p)=(E_d-p^2/M)\varphi_l(p),\quad l=0,2\ , \tag{11}$$

where $\varphi_0(p)$ and $\varphi_2(p)$ are the S and D wave components of the deuteron wave function. The relativistic form factors $g_j^{\alpha_j(p_{lj})}$ are related to the nonrelativistic ones by means of the minimal relativity transformation,[29] as

$$g_j^{\alpha_j}(p_j)=2\sqrt{M}\,(M^2+p^2)^{1/4}h_{lj}(p_j)\ . \tag{12}$$

In the case of the nucleon-nucleon $^1S_0$ channel, a similar minimal relativity transformation[11,12] was applied to the rank-one separable representation of the Paris potential by the so-called Ernst-Shakin-Thaler (PEST1) approximation.[30] It should be pointed out that there are no free parameters in this theory outside the parameter Λ, which has been fixed at 1 GeV/c, since it has a very weak influence in the differential cross section.

III. EXPERIMENTAL TECHNIQUE

For a specific incident particle energy, it is sufficient to observe two of the three final-state particles at well-defined angles and to measure one of their energies in order to determine any of the kinematic variables for any of the reaction products, including the third (undetected) particle. This is the minimum requirement for a kinematically complete experiment. In order to cover a relatively large bite of the accessible three-body phase space simultaneously, an arrangement of counters previously used in the study of pion-deuteron elastic scattering[8] was used with a suitably modified electronics

configuration. In the earlier two-body reaction studies at TRIUMF, a scattered pion could be observed in one of six symmetric arms, and a coincident deuteron could be observed in one of six complementary arms suitably located. For the present three-body application the electronics configuration recorded an event when a pion was observed in any of the six symmetric pion arms, and a coincident particle was detected in any of the six arms on the opposite side of the beam. Details of this arrangement (the time-of-flight spectrometer) have been described elsewhere.[8]

As the name indicates, the counters were arranged for optimum timing for any of the arms relative to the signal from the second of two in-beam scintillators, that defined the timing of the event presented to the computer as well as the start timing of all of the time to digital convertors (TDC) and defined which pions in the beam were accepted. The experiment was performed at the $M11$ medium-energy pion channel at TRIUMF. The detectors were arranged at a variety of horizontal angles with their centers in the horizontal plane. The out-of-plane angle could be inferred from the difference in timing of signals from the two ends of any one detector, which were both included in the data written to tape in addition to the hardware meantime of the two ends. With this time-of-flight technique the ability to cover a broad region of phase space simultaneously was possible at the expense of the high resolution offered by an alternative arrangement employing some form of magnetic spectrometer as was used in the Rice University experiments. The time-of-flight binning in this experiment, 450 psec, leads to a nonlinear momentum binning from about 10 MeV/c for 200 MeV/c protons to 30 MeV/c for 500 MeV/c protons. For a particular path length, L, and energy, E, the momentum bite corresponding to a fixed time of flight bite, dT, is

$$dP=(EP^2/M^2)(dT/Lc^2)\ .$$

The $M11$ pion beam uses a differential degrading technique to reduce the fraction of contaminating protons in the beam. In addition to the lower level thresholds set on the in-beam counters to detect pions, an upper level threshold was applied to avoid counting the few residual incident protons. The beam coincidence timing was arranged to discriminate against muons and electrons in the beam. The pion rate was normally near 3 MHz, which with the TRIUMF beam structure leads to a significant fraction of beam bursts with two pions which can not be distinguished from single pions. For these cases the scaling of the beam is not correct and a factor S_π, which reduces the yield per incident pion (by 6% at this beam rate), is required to correct for instances when two pions struck the target within one beam burst. The momentum resolution of the incident beam, defined with a set of horizontal slits, was $dP/P=0.01$.

Targets used in this experiment included polythene, $(CH_2)_n$, liquid deuterium, and an empty liquid target vessel for background measurements. The cryogenic target was rectangular in cross section with the liquid surfaces kept flat by a thin region of pressurized gas. The areal density of deuterons in the target was 3.58×10^{22} deuterons per cm^2. All three targets were mounted on the same assembly within the cryostat and any target could be moved into the beam easily so that frequent calibration and background runs were included with every set of foreground runs. Data were collected in sequences of five runs with the deuterium target, one run with the background target, and one run with the calibration target In each sequence about 1.2 million events were written to tape and seven independent sequences were completed.

IV. DATA ANLAYSIS

The 12 arms were arranged in a matrix configuration, with the smallest pion angle (arm pion A) through largest (pion F) located at complementary angles to the largest proton angle (arm proton A) through to the smallest proton angle (proton F), so that the diagonal combinations (pion-A in coincidence with proton A etc.) of the angle matrix were suitable for measurements of the pion-proton elastic scattering reaction. For these diagonal angle combinations, the time of flight to each arm, in TDC units, was simply related to the calculated time of flight, in nanoseconds, for the two-body reaction.

In order to ensure that the absolute time-of-flight calibration derived from the preceding two-body measurements was also appropriate for coincidences from the three-body final-state including angle pairs off the diagonal of the angle pair matrix, three sets of synchronizing constants were determined from the data as follows. The first set of constants, intended to synchronize the timing for any event independent of which of the six look at me (LAM) coincidences that caused the event to be recorded, was determined from the centroid of the time of flight between the first and second in-beam counters, as seen from the six different LAM types. The other two sets of constants were determined from numerous two-body measurements, where each pair of arms was positioned at several settings of complementary angles for the two-body reaction. With all 18 constants in use, the absolute time of flight for any pion or for any proton arm could be determined, regardless of which angle pair caused the LAM.

The first cut in the event-by-event analysis of the data, is a one-dimensional cut applied on the calculated displacement in TDC units from the nearest point on the kinematical locus of pion versus proton time of flight for the three-body reaction. This cut distinguishes the three-body reaction of interest from some of the two-body final-state reactions, and from three-body reactions with two final-state protons detected (as one finds in the reaction $\pi^+d\rightarrow\pi^0pp$).

Within the proton arm the pulse-height information from the three counters may be used to plot a typical dE vs E graph. A two-dimensional cut applied to this graph enables separation of nearly all final-state deuterons from the competing pion-deuteron elastic scattering reaction. For a few of the angle pairs, with large pion angles, the scattered deuterons have sufficient energy to pass through all three counters leaving no way to separate them from the protons of interest, forcing the removal of a few of the points from the final cross-section distributions. With this two-dimensional cut, it was possible to remove very

fast protons arising from pion absorption and pions that would contribute to random events or events with the pion and proton arm roles reversed.

Within the pion arm, a one-dimensional cut on the pulse height was applied to select pions from the breakup reaction and further remove protons from the absorption reaction or breakup reversed events (a proton into the pion arm and vice versa).

The results of these event-by-event cuts were compiled as histograms of the time-of-flight difference between the pion and proton arms for runs with both full target cell and empty target cell. The time-of-flight difference was chosen to eliminate any time-of-flight jitter that could in principle be introduced from the second in-beam counter, on which the timing for each type of LAM was based. Final histograms of this quantity for runs with the liquid deuterium were then translated into histograms of the absolute time of flight from a table of kinematical time-of-flight differences versus the absolute time of flight of the protons for the breakup reaction.

Cross sections were determined for groups of five histogram bins of the time-of-flight distributions, corresponding to a total time-of-flight bin of 440 psec as follows:

$$\frac{d^3\sigma}{d\Omega_\pi d\Omega_p dP_p} = \frac{\text{yield} \times S_\pi}{dP_p N_\pi N_{tgt} \epsilon_\pi \delta\Omega_\pi \epsilon_p \delta\Omega_p \epsilon_{lt}} ,$$

where the doubles corrections, S_π, has been discussed above, dP is the variable momentum bin calculated from the fixed time-of-flight bin, ϵ_{lt} is the computer live time correction, ϵ_π is a correction for pion decays in flight, and ϵ_p is a correction for the fraction of protons which fall out of the two-dimensional EdE cut due to reactions (mostly p,n) in the proton counters. This cross-section distribution as a function of the absolute proton time of flight was then simply mapped into a distribution expressed as a function of proton momentum by straightforward kinematics.

The initial distributions of cross section as a function of proton momentum suffer from a nonlinear momentum bin width, dP, and correspond to finite horizontal and vertical angular bins for both the proton and pion. It was decided that the comparison with theory could best be accomplished if the data, which represent the experimental average over all of these bin widths, were corrected to correspond more closely to the cross section at the center of the bin in each of these dimensions. Since the cross section is known to vary rapidly with momentum and angle, these corrections are significant and will be discussed in some detail.

The momentum distributions for a particular set of pion and proton angles were typically fit with up to nine parameters (a combination of a Gaussian, a Lorentzian, and a quadratic function). Each momentum bin was then divided up into several subbins, over which the fitted distribution was integrated and an average determined. On the sides of the momentum peak, this average is greater than the value of the distribution at the center of the bin, so the experimental cross section for the bin was corrected by the ratio of the fitted value at the center of the bin to the average value over the whole bin. These corrections reduce the cross sections a few percent on the low-momentum side of the peaked distributions, and up to 20% on the high-momentum side (where the momentum bins are larger) of the peaked distributions. In the region of the peak, for strongly peaked distributions, the cross section was corrected upwards, by at most 2%. In distributions which had no significant peak, this correction clearly was insignificant.

After correcting the momentum distributions for the momentum binning, the distributions were integrated and the integral plotted against both the pion and proton horizontal angles. These angular distributions of momentum integrated cross sections were then separately fit with five parameters (combination of a Gaussian and linear functions). The fitted distributions were used in a similar fashion as the momentum fitted distributions to extract a correction factor for each of the horizontal finite angle bin widths. The product of the two factors, which was applied to the entire momentum distribution at each pion-proton angle pair, typically increased the data by a few percent when the angles were near those for free pion-proton elastic scattering, and decreased the data by a few percent in angular regions away from the maxima.

The first counter in the proton arms and the second counter in the pion arms were arranged for optimal timing resolution with a tube at each end of the scintillator to average out the time jitter due to the location along the counter where the detected particle struck. Clearly by recording both of these timing signals from each counter enabled a software meantime could be calculated to check the hardware meantime signal, which was also written to tape. In addition the out of plane position was determined from the difference in timing from the two ends of any particular timing counter. The average arrival time of a light pulse at the phototube depends upon the path length along the scintillator, and on the ratio of the direct to the reflected light within the plastic. In order to confirm our understanding of the out-of-plane distribution extracted in this fashion a brief test was conducted, in which a small detector in coincidence with one of the timing counters, was moved along the longer counter and the position as a function of the time-of-flight difference to the two ends was mapped out. In the data analysis an estimated distribution, truncated at the effective edges of the counter, was convoluted with the time-of-flight resolution and iterated until a satisfactory comparison with the experimentally determined time-of-flight difference was achieved. The estimated or input distributions were then integrated and compared with the value at the center of the distribution as was done for the other corrections already discussed. In regions where the momentum distribution was also strongly peaked, it turned out that the out-of-plane distribution was strongly peaked and the data were typically increased by 20–40%. In regions away from the free scattering angles, the corrections were smaller and those for the out of plane distribution were much less significant. Typical distributions of the relative yield as a function of the vertical position along a proton counter at 42° are shown for six different pion angles in Fig. 1.

Data from every data sequence (including runs with

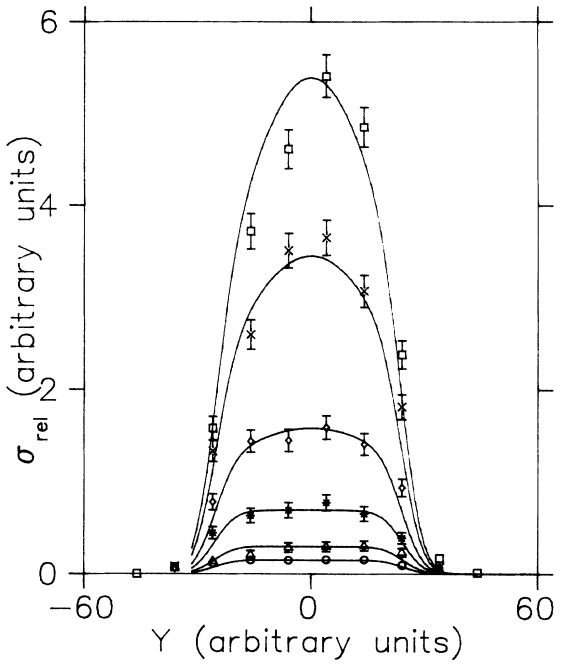

FIG. 1. Distributions of relative cross sections for pion-deuteron breakup as a function of the proton vertical angle for final-state pions detected at a horizontal angle of 75° □, 37.8°×, 32.8°◇, 27.5°*, 20.2°△, 12.5°○ compared with the empirical distribution as discussed in the text.

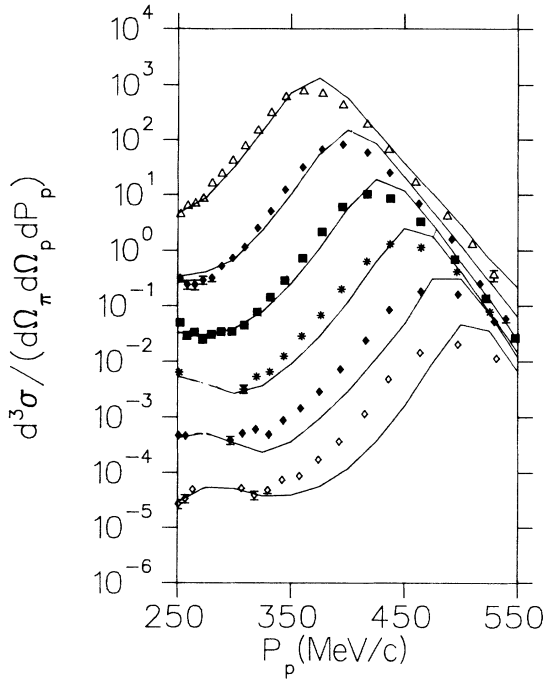

FIG. 2. Distributions of the differential cross sections for pion deuteron breakup as a function of the proton momentum, expressed in μbsr^{-2} (MeV/c)$^{-1}$ for six different angle pairs corresponding to free pion-proton elastic scattering compared with Fadeev calculations. Each successive distribution has been divided by an additional factor of 10 to further displace the curves. Data plotted with Δ correspond to $\theta_\pi = 75°$, $\theta_p = 42.8°$; with ♦ to 85.0°, 37.8°, with ■ to 95.0°, 32.8°, with * to 107.5°, 27.5°; with ⧫ to 125.0° 20.2°; with ◇ to 145.0°, 12.5°.

the liquid deuterium target, background empty target cell, and calibration runs) were analyzed separately, and then the results from all the data sets were averaged together and a bin by bin standard deviation determined. In this way the quoted uncertainty also reflects any small timing shifts that may have occurred between calibrations and different data sets.

V. RESULTS AND DISCUSSION

The cross sections for the pion deuteron breakup reaction at 228 MeV are shown in Fig. 2 for six cases where both pion and proton angles correspond to free pion-proton elastic scattering angles. Representative cross sections for a variety of proton angles and three pion angles are shown in Figs. 3–5. The uncertainty due to statistics including background subtraction has been plotted for those points where the error bar is larger than the plotting symbol. The general trend of the data is reproduced in the few-body calculation with varying degrees of success in different kinematic regions of phase space. Tables of cross sections corresponding to all 36 angle pairs were deemed too bulky to be included in this paper, but are available from the authors.

At the most forward pion angle studied (75°, see Fig. 3) the data with angles closest to those for free pion-proton elastic scattering are well described in much of the spectrum except, surprisingly, in the region of quasifree scattering (spectator neutron momentum minimal) where the data is below the theoretical curve by about 30%. As one considers data taken with proton angles progressively smaller than those for free pion-proton elastic scattering the distributions become much less peaked and discrepancies between theory and experiment develop in the low-proton-momentum region, where the data lie above the theory; and in the higher-proton-momentum region, where the data fall below the calculation.

These differences with respect to the theoretical calculation become more pronounced as one considers data taken for the same range of proton angles and larger pion angles (see Figs. 4 and 5). At the largest pion angles the agreement is the worst, with large differences for a wide variety of proton momenta.

Of the 36 angle pairs where data was obtained there are 6 angle pairs which were deliberately chosen to repeat measurements in the earlier SIN experiment. These measurements not only allow a check between the two experiments but also a comparison between data analyzed with rather different approaches. In the SIN work the data were fitted with a multidimensional parametrization, including both pion and proton horizontal scattering angles and the proton momentum distribution, and several correlations between these quantities. From this global fit the data were corrected in such a way as to represent

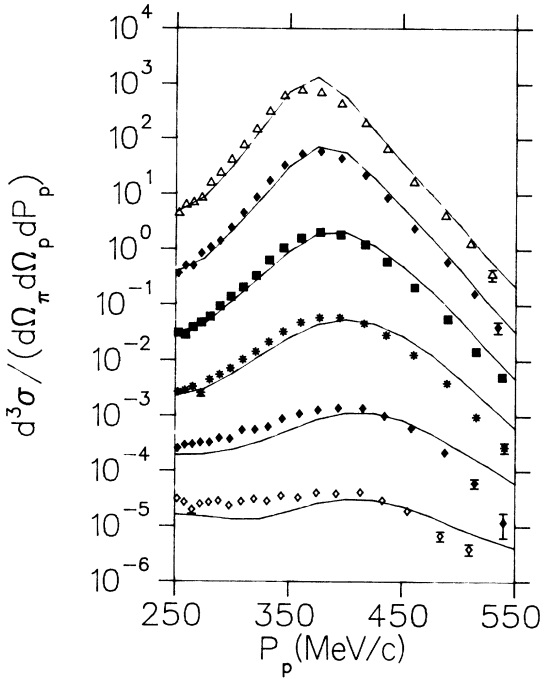

FIG. 3. Distributions of the differential cross sections for pion-deuteron breakup as a function of the proton momentum, expressed in μbsr^{-2} (MeV/c)$^{-1}$ for θ_π=75° and six different proton angles compared with Fadeev calculations. Each successive distribution has been divided by an additional factor of 10 to further displace the curves. Data plotted with Δ correspond to θ_p=42.8°; with ♦ to 37.8°, with ■ to 32.8°; with * to 27.5°; with ⊕ to 20.2°; with ◇ to 12.5°.

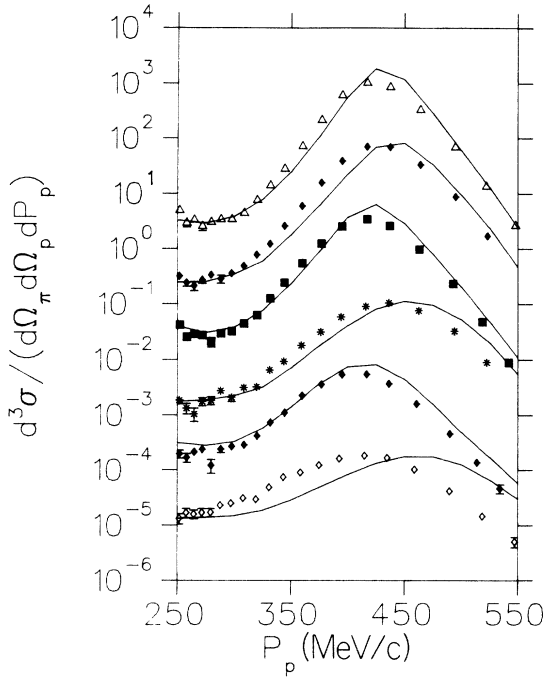

FIG. 4. Distributions of the differential cross sections for pion-deuteron breakup as a function of the proton momentum, expressed in μbsr^{-2} (MeV/c)$^{-1}$ for θ_π=95° and six different proton angles compared with Fadeev calculations. Each successive distribution has been divided by an additional factor of 10 to further displace the curves. Data plotted with △ correspond to θ_p=32.8°; with ♦ to 27.5°, with ■ to 37.8°; with * to 20.2°; with ⊕ to 42.9°; with ◇ to 12.5°.

the cross section at the middle of the horizontal angle and momentum bites, as opposed to the experimentally averaged value over the same bites. Since no out-of-plane information could be extracted from the SIN data, a correction was modeled and recently applied to the data. As already discussed, the corresponding corrections to this experiment were made independently with separate fits over each dimension and it is assumed that the correlations between dimensions are not important. An explicit out-of-plane correction was determining from the data and has also been applied. For all six comparison cases the two experiments are in good agreement in the regions of low proton momentum where the final state NN interaction is most important. In the quasifree scattering region, where the sensitivity to the out-of-plane correction is greatest, the corrected SIN data is higher than this new TRIUMF data in four cases (see for example Fig. 6) and in better agreement in the remaining two cases (see Fig. 7 for example). In the region of proton momentum above quasifree scattering the new data typically lie somewhat above the SIN results.

VI. CONCLUSIONS

These new data for the pion-deuteron breakup reaction were measured with the hope that, together with the complementary data from the Karlsruhe and Rice experiments, and with the experience gleaned from polarization studies of the coupled two-body reactions, that a new evaluation of the completeness of modern theoretical treatments of the πNN system could be evaluated. Unfortunately, several of the major proponents of suitable calculations have not yet included calculations of the cross sections for the three-body final states limiting the ability to ascertain the importance, for example, of the different approaches to the relativistic aspects of the theory. Extensions of the earlier efforts which have been focused on the two-body reactions are urgently required.

A variety of experiments have been conducted to evaluate the contributions of final-state interactions to the cross section. In the case of pion-deuteron breakup one expects such contributions when the final-state neutron and proton momenta are comparable. With 228-MeV incident pions this occurs in the region of proton momenta below 300 MeV/c. At 294 List *et al.*[18] have found small peaks in the cross section in this kinematical region, and although one does not find peaks in the new data at 228 MeV, it is clear that the cross section falls off much slower on the low-momentum side of the quasifree scattering peak than on the high-momentum side. At forward pion angles the data show a final-state interaction enhancement somewhat greater than the theoretical

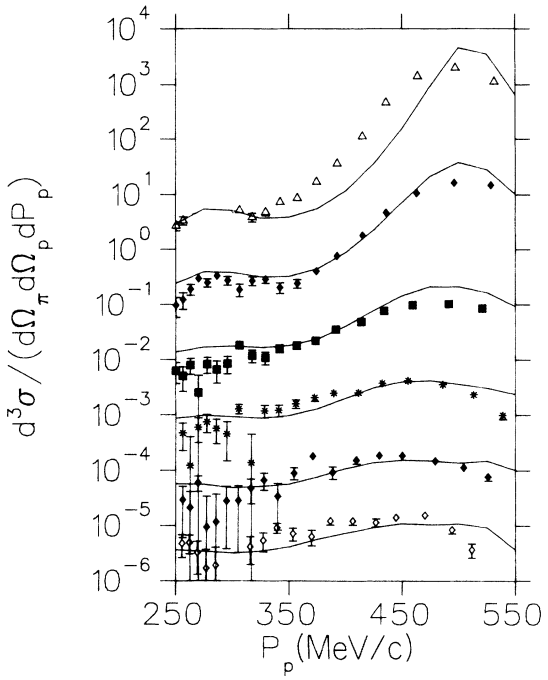

FIG. 5. Distributions of the differential cross sections for pion-deuteron breakup as a function of the proton momentum, expressed in μbsr^{-2} (MeV/c)$^{-1}$ for $\theta_\pi = 145°$ and six different proton angles compared with Fadeev calculations. Each successive distribution has been divided by an additional factor of 10 to further displace the curves. Data plotted with Δ correspond to $\theta_p = 12.5°$; with ♦ to 20.2°; with ♦ to 27.5°; with * to 32.8°; with ⊕ to 37.8°; with ◇ to 42.9°.

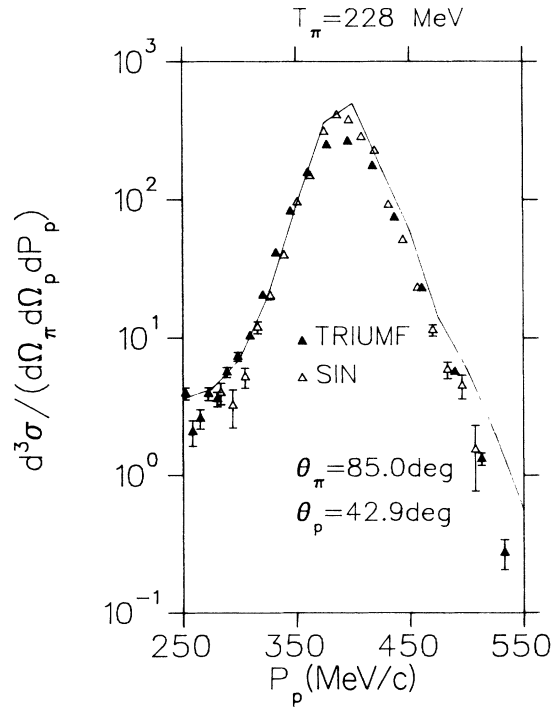

FIG. 6. Comparison of the momentum distributions of differential cross sections between this experiment and the Karlsruhe results for the angle pair indicated, corrected for the out-of-plane detector acceptance. The curve is the Faddeev calculation.

calculations predict. At the larger pion angles, distributions with proton angles near the free scattering angles are missing some points in the region of the final-state interaction, because the technique used did not allow clear deuteron versus proton separation. In summary, one finds a clear indication of peaking in the final-state interaction region at 294 MeV, and only a flattening of the distribution at 228 MeV. Measurements at several energies will clarify the importance of this aspect of the interaction, which is reflected in the Faddeev calculations.

In their work, Pancella *et al.* have integrated the three-body results in such a way as to derive a single differential cross section for the delta production reaction, $\pi + d \rightarrow n + \Delta^{++}$, or presented triple differential cross sections with respect to pion rather than proton momentum making direct comparisons between the experiments awkward. One might expect that delta formation would be reflected in a peaked cross section in the distributions as a function of final-state proton momentum because the onset of the delta has a dramatic effect in the cross sections for the related NN to πNN reaction. In the data presented here, one typically finds that in the kinematical region where the invariant mass of the final-state pion and proton coincide with a delta (the high-momentum region) the cross sections are normally falling rapidly without any obvious peaks. At the most forward pion angles studied and for proton angles smaller than those for elastic scattering, the delta kinematical region tends to coincide with the quasifree scattering region,

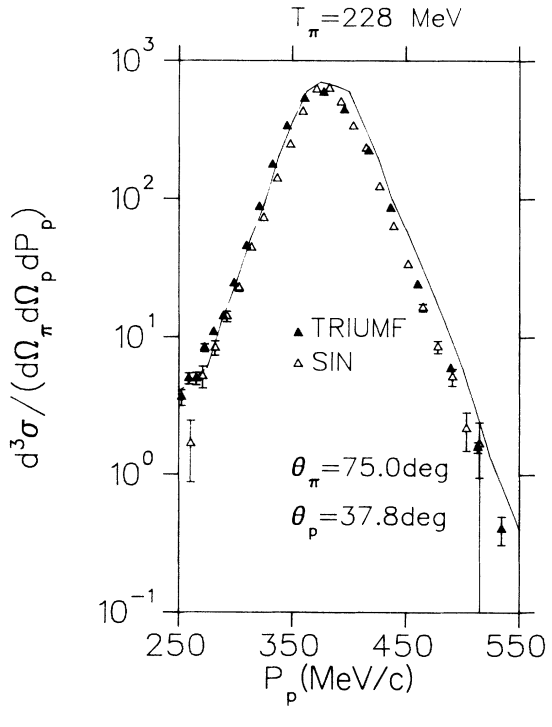

FIG. 7. Comparison of the momentum distributions of differential cross sections between this experiment and the Karlsruhe results for the angle pair indicated, corrected for the out-of-plane detector acceptance. The curve is the Faddeev calculation.

where one would expect a peak in any case. Typically in the high-proton-momentum region, both the Karlsruhe and these experiments indicate that the theoretical result is too high, with the disagreement between theory and the Karlsruhe result somewhat greater. As for the final-state interaction region, data at a variety of energies, above and below the delta resonance, can more effectively address this question.

It is found in both this work and in the Pancella results that the comparison with theory is not satisfactory in the region of the quasifree scattering peak. This was less true in the comparison of the theory with the first Karlsruhe experiments, however the application of the out of plane correction in that data (which are most significant in the quasifree scattering region) was not based directly on the data, as was done in the present work. These experimental differences could be better addressed in an experiment using small vertical acceptance counters to measure cross sections at a few points; or in an experiment with the ability to measure a complete out-of-plane distribution accurately. There is no explanation at present why the quasifree scattering region is not well described in the Fadeev calculations. The failure of the theory to describe the data at larger pion angles, which is also true for a variety of observables in some of the coupled two-body reaction channels, may well be an indication of the need to consider intermediate states with pion delta and perhaps even delta-delta interactions explicitly included.

ACKNOWLEDGMENTS

We gratefully acknowledge the contributions of the TRIUMF technical, offline computing, and operations staffs, as well as financial support from the Natural Sciences and Engineering Research Council of Canada. We thank Mr. B. Elrick for his assistance in preparing figures of some of the data. One of us (H.G.) was supported by the German Federal Ministry for Research and Technology (BMFT) under Contract No. MEP0234HAA.

---

*Present address: IUCF, Bloomington, IN 47408.

†Present address: Chemische Werke Bayer, Leverkusen, Federal Republic of Germany.

‡On leave from Escuela Superior de Fisica y Matematicas, Instituto Politecnico Nacional, Mexico 14 D.F., Mexico.

[1]G. H. Lamot, J. L. Perrot, C. Fayard, and T. Mizutani, Phys. Rev. C **35**, 239 (1987).

[2]B. Blankleider and I. R. Afnan, Phys. Rev. C **24**, 1572 (1981).

[3]I. R. Afnan and R. J. McLeod, Phys. Rev. C **31**, 1821 (1985).

[4]A. S. Rinat and Y. Starkand, Nucl. Phys. **A397**, 381 (1983).

[5]H. Garcilazo, Phys. Rev. Lett. **45**, 780 (1980); Phys. Lett. **99B**, 195 (1981); Phys. Rev. C **26**, 2685 (1982).

[6]H. Garcilazo, Phys. Rev. Lett. **53**, 652 (1984).

[7]C. Ottermann, E. T. Boschitz, W. Gyles, W. List, R. Tacik, R. R. Johnson, G. R. Smith, and E. L. Mathie, Phys. Rev. C **32**, 928 (1985).

[8]G. R. Smith *et al.*, Phys. Rev. C **38**, 251 (1988).

[9]G. R. Smith *et al.*, Phys. Rev. C **30**, 980 (1984).

[10]E. L. Mathie, G. R. Smith, E. T. Boschitz, and J. Hoftiezer, Z. Phys. A **313**, 105 (1983).

[11]J. H. Hoftiezer *et al.*, Phys. Lett. B **88**, 73 (1979).

[12]J. H. Hoftiezer *et al.*, Phys. Rev. C **23**, 407 (1981).

[13]A. Matsuyama, Nucl. Phys. **A379**, 415 (1982).

[14]H. Garcilazo, Phys. Rev. Lett. **48**, 577 (1982).

[15]E. L. Mathie, G. R. Smith, E. T. Boschitz, W. Gyles, C. R. Ottermann, S. Mango, J. A. Konter, A. Matsuyama, R. R. Johnson, and R. Olszewski, Phys. Lett. B **154**, 28 (1985).

[16]W. Gyles, E. T. Boschitz, H. Garcilazo, E. L. Mathie, C. R. Ottermann, S. Mango, J. A. Konter, A. Matsuyama, R. R. Johnson, and R. Olszewski, Phys. Rev. C **33**, 595 (1986).

[17]W. Gyles, E. T. Boschitz, H. Garcilazo, W. List, E. L. Mathie, C. R. Ottermann, G. R. Smith, R. Tacik, and R. R. Johnson, Phys. Rev. C **33**, 583 (1986).

[18]W. List, E. T. Boschitz, H. Garcilazo, W. Gyles, C. R. Ottermann, R. Tacik, M. Wessler, and U. Wiedner, Phys. Rev. C **37**, 1587 (1988).

[19]W. List, E. T. Boschitz, H. Garcilazo, W. Gyles, C. R. Ottermann, R. Tacik, S. Mango, J. A. Konter, B. van den Brandt, and G. R. Smith, Phys. Rev. C **37**, 1594 (1988).

[20]P. V. Pancella *et al.*, Phys. Rev. C **38**, 2716 (1988).

[21]H. Garcilazo, J. Math. Phys. **27**, 2576 (1986).

[22]G. C. Wick, Ann. Phys. (N.Y.) **18**, 65 (1962).

[23]H. Garcilazo, Phys. Rev. C **37**, 2022 (1988).

[24]H. Neilsen and G. C. Oades, Nucl. Phys. B **49**, 573 (1972).

[25]H. Neilsen, J. L. Petersen, and E. Pietarinen, Nucl. Phys. B **22**, 525 (1970).

[26]H. Garcilazo, Phys. Rev. C **15**, 1667 (1977).

[27]E. Harms, Phys. Rev. C **1**, 1667 (1970).

[28]M. Lacombe, B. Loiseau, R. Vinh Mau, J. Côté, P. Pirés, and R. de Tourreil, Phys. Lett. B **101**, 139 (1981).

[29]G. E. Brown and A. D. Jackson, *The Nucleon Nucleon Interaction* (North-Holland, Amsterdam, 1976).

[30]J. Heidenbauer and W. Plessas, Phys. Rev. C **30**, 1822 (1984).